

Hyperspectral pan-sharpening: a variational convex constrained formulation to impose parallel level lines, solved with ADMM

Alexis Huck, François de Vieilleville, Pierre Weiss and Manuel Grizonnet

Abstract—In this paper, we address the issue of hyperspectral pan-sharpening, which consists in fusing a (low spatial resolution) hyperspectral image HX and a (high spatial resolution) panchromatic image P to obtain a high spatial resolution hyperspectral image. The problem is addressed under a variational convex constrained formulation. The objective favors high resolution spectral bands with level lines parallel to those of the panchromatic image. This term is balanced with a total variation term as regularizer. Fit-to-P data and fit-to-HX data constraints are effectively considered as mathematical constraints, which depend on the statistics of the data noise measurements. The developed Alternating Direction Method of Multipliers (ADMM) optimization scheme enables us to solve this problem efficiently despite the non differentiability and the huge number of unknowns.

Index Terms—hyperspectral, fusion, pan-sharpening, ADMM

I. INTRODUCTION

High spectral resolution of hyperspectral imaging sensors generally implies concession on spatial resolution due to optics/photonics and cost considerations.

If high spatial resolution panchromatic data are available, hyperspectral pan-sharpening can significantly help to improve the spatial resolution of sensed hyperspectral images.

In the last three decades, pan-sharpening approaches were dedicated to multispectral data. The earliest methods were based on specific *spectral-space transforms* such as the Hue-Intensity-Saturation (HIS) transform or the Principal Component Analysis (PCA) Transform. More recently, spatial frequency based approaches such as the High Pass Filter (HPF) method exploiting multiscale spatial analysis [1] provided improved results. The multiscale spatial analysis framework generally offers very time efficient performance but lacks flexibility to consider some prior knowledge about “physics of scene and sensor” (the sensors Modulation Transfer Function (MTF), sensor noise or any prior information). This aspect has been a limitation for application to hyperspectral pan-sharpening. Thus, recent methods are generally based on variational [2] or bayesian [3] formulations. In particular, in [2], the authors have proposed to consider a term based on the topographic properties of the panchromatic image. This idea stems from [4] where the authors show that most geometrical information of an optical image lies in the set of its gray level-lines.

The proposed algorithm includes three novelties: 1. we propose a constrained convex formulation where the constraints are the fit-to-data terms. This enables to easily tune the related parameters which are the (supposed) known noise variances of the sensors. 2. The proposed minimization algorithm is based on the ADMM. It handles the non differentiability, constraints and special structures of the linear transforms in an efficient way. 3. The formulation takes the MTF (Modulation Transfer Function) into account, which helps refining the fit-to-hyperspectral-data constraint. This is favorable to high spectral fidelity in pan-sharpened hypersepectral data.

II. PROBLEM FORMULATION

In this paper, we rearrange (hyperspectral) images into vectors in order to allow writing matrix-vector products. Let

$$x = \begin{pmatrix} x_1 \\ \vdots \\ x_L \end{pmatrix} \in \mathbb{R}^{LM} \text{ and } u = \begin{pmatrix} u_1 \\ \vdots \\ u_L \end{pmatrix} \in \mathbb{R}^{LN} \text{ denote}$$

the low spatial resolution (LR) measured hyperspectral image and the (unknown) high spatial resolution hyperspectral image respectively. The integers L and M represent the number of spectral bands and the number of spectral pixels in the low resolution image, respectively. We let $p \in \mathbb{R}^N$ denote the rearranged panchromatic measured image, where $N = q^2 \times M$ and $q \geq 1$ denotes the resolution factor between the low and high resolution images. The linear projection operator which returns the l^{th} spectral band is denoted π_l . Then, $x_l = \pi_l x \in \mathbb{R}^M$ and $u_l = \pi_l u \in \mathbb{R}^N$ are the l^{th} spectral bands of x and u respectively.

A model formulation for any spectral band l of the hyperspectral measurements is given by

$$x_l = \mathbf{D}_s \mathbf{H}_s u_l + n_{x_l}. \quad (1)$$

The linear operator $\mathbf{H}_s \in \mathbb{R}^{N \times N}$ represents the spatial convolution with the spatial Point Spread Function of the hyperspectral sensor. The linear operator $\mathbf{D}_s \in \mathbb{R}^{M \times N}$ is a downsampling operator that preserves 1 every q pixels in the horizontal and vertical directions. Some additive sensor noise is considered in the vector n_{x_l} . We assume that $n_{x_l} \sim \mathcal{N}(0, \sigma_{x_l}^2)$ where $\sigma_{x_l}^2$ is the noise variance of the l^{th} measured hyperspectral band.

A model formulation for the panchromatic image acquisition process is given by

$$p = \mathbf{G}u + n_p \quad (2)$$

A. Huck and F. De Vieilleville are with Magellium, Toulouse, France.
P. Weiss is with ITAV-USR3505, universit  de Toulouse, France.
M. Grizonnet is with CNES, Toulouse, France.

where $\mathbf{G} \in \mathbb{R}^{N \times LN}$ is a linear operator which linearly and positively combines the spectral bands with weights equal to the samples of the sensitivity spectral pattern of the panchromatic image. The noise of the measured panchromatic image is denoted $n_p \sim \mathcal{N}(0, \sigma_p^2)$.

Analogously to [2], we will exploit the fact that the different spectral bands of hyperspectral images approximately share the same level lines. Such a knowledge can be integrated by comparing the gradient of the panchromatic data with the gradient of each hyperspectral image channel. A simple way to measure the discrepancy between the normal fields consist of using the function f below

$$f(u) = \sum_{l=1}^L \sum_{i=1}^N \left| \left\langle \nabla u_l(i), \frac{\nabla^\perp p(i)}{\|\nabla p(i)\|_2} \right\rangle_{\mathbb{R}^2} \right| \quad (3)$$

where $\nabla = [\partial_h^\top, \partial_v^\top]^\top : \mathbb{R}^N \rightarrow \mathbb{R}^N \times \mathbb{R}^N$ is the standard discrete gradient operator, ∂_h and ∂_v are the horizontal and vertical gradient operators respectively, $\langle \cdot, \cdot \rangle_{\mathbb{R}^2}$ is the standard Euclidian dot product in \mathbb{R}^2 and $\|\cdot\|_2$ the associated L_2 norm. The operator $\nabla^\perp = [-\partial_v^\top, \partial_h^\top]^\top : \mathbb{R}^N \rightarrow \mathbb{R}^N \times \mathbb{R}^N$ returns for each pixel a vector orthogonal to the gradient. Functional f has many attractive properties: it is convex in u and it can be shown to have a meaning in the continuous setting for bounded variation functions.

In natural scenes, the gradient can be very low in image areas corresponding to homogeneous radiometry of the scene. In such a case, f does not provide much information and an additional regularizing term should be added in the variational formulation. In this work, we use a standard total variation regularizer [5], commonly used for such purposes and adapted in Eq. 4 to multiband images

$$TV(u) = \sum_{l=1}^L \sum_{i=1}^N \|(\nabla u_l)(i)\|_2 \quad (4)$$

where $\|\cdot\|_2$ is L_2 -norm in \mathbb{R}^2 . The proposed variational formulation for the hyperspectral pan-sharpening problem is as follows:

$$\begin{aligned} \hat{u} &= \underset{u}{\operatorname{argmin}} \gamma f(u) + (1 - \gamma)TV(u) \quad (5) \\ \text{s.t.} \quad &\|x_l - \mathbf{D}\mathbf{H}_s u_l\|_2^2 \leq M\sigma_{x_l}^2, \forall l \in [1, \dots, L] \\ &\|p - \mathbf{G}u\|_2^2 \leq N\sigma_p^2 \end{aligned}$$

where $\|\cdot\|_2$ denotes the L_2 norm in \mathbb{R}^M or \mathbb{R}^N . In this formulation, $\gamma \in [0, 1]$ fixes a balance between the two terms f and TV . The fit-to-data terms are constraints deriving from the physical models (Eq. 1 and 2). The parameters $\{\sigma_{x_l}\}_{l \in \{1, \dots, L\}}$ and σ_p can be *a priori* given or estimated, which is a strong asset of the variational constrained formulation.

III. ADMM BASED OPTIMIZATION

The proposed algorithm is called TVLCSP (for Total Variation iso-gray Level-set Curves Spectral Pattern) and its pseudo-code is given in the procedure TVLCSP. A variant (called TVLC) not considering the sensitivity spectral and fit-to-panchromatic data has been developed but is not presented here.

```

1: procedure TVLCSP( $x, p, \sigma_x, \sigma_p, \alpha, \beta$ )
2:   # Initialization
3:    $\lambda \leftarrow 0$  ▷ a vector of zeroes.
4:    $y_1 \leftarrow [\uparrow x^\top, \uparrow x^\top]^\top$ ,  $y_2 \leftarrow [\uparrow x^\top, \uparrow x^\top]^\top$ ,
5:    $y_3 \leftarrow \uparrow x$ ,  $y_4 \leftarrow p$ 
6:   # Iterative scheme
7:   while stop condition not met do
8:     for all  $l \in \{1, \dots, L\}$  do
9:        $z_{1,l} \leftarrow \nabla u^l - \frac{\lambda_1^l}{\beta}$ 
10:       $y_1^l \leftarrow \frac{z_1^l}{\|z_1^l\|_{2,\mathbb{R}^2}} \cdot \max\left(\|z_1^l\|_{2,\mathbb{R}^2} - \frac{\gamma}{\beta}, 0\right)$ 
11:       $\epsilon \leftarrow \langle y_2^l, \eta \rangle_{\mathbb{R}^2}$  ▷ where  $\eta = \frac{\nabla^\perp p}{\|\nabla p\|_2}$ 
12:      if  $\epsilon \neq 0$  then
13:         $y_2^l \leftarrow \nabla u^l - \frac{1}{\beta}(\lambda_2^l + (1 - \gamma)\operatorname{sign}(\epsilon)\eta)$ 
14:      else
15:         $z_2^l \leftarrow \nabla u - \frac{\lambda_2^l}{\beta}$ 
16:         $\alpha \leftarrow \beta \frac{\langle z_2^l, \eta \rangle_{\mathbb{R}^2}}{(1 - \gamma)\|\eta\|_{2,\mathbb{R}^2}^2}$ 
17:         $y_2^l \leftarrow \left(\mathbb{1} - \frac{1 - \gamma}{\beta}\alpha\right) \cdot z_2^l$ 
18:      end if
19:       $z_3^l \leftarrow \frac{\lambda_3^l}{\beta} - \mathbf{H}_s u$ 
20:      if  $\|x^l - \mathbf{D}_s \mathbf{H}_s u^l\|_2^2 \leq M\sigma_x^2$  then
21:         $y_3^l \leftarrow z_3^l$ 
22:      else
23:         $\delta \leftarrow \frac{\|x^l - \mathbf{D}_s \mathbf{H}_s u^l\|_2 - \sqrt{M}\sigma_x}{\sqrt{M}\sigma_x}$ 
24:         $y_3^l \leftarrow \left[\operatorname{Id} - \frac{\delta}{\beta + \delta} \mathbf{D}_s^\top \mathbf{D}_s\right] z_3^l + \frac{\delta}{\beta + \delta} \mathbf{D}_s^\top x$ 
25:      end if
26:    end for
27:     $z_4 \leftarrow \frac{\lambda_4}{\beta} - \mathbf{H}_\lambda u$ 
28:    if  $\|p - \mathbf{D}_\lambda \mathbf{H}_\lambda u\|_2^2 \leq N\sigma_p^2$  then
29:       $y_4 \leftarrow z_4$ 
30:    else
31:       $\delta \leftarrow \frac{\|p - \mathbf{D}_\lambda \mathbf{H}_\lambda u\|_2 - \sqrt{N}\sigma_p}{\sqrt{N}\sigma_p}$ 
32:       $y_4 \leftarrow \left[\operatorname{Id} - \frac{\delta}{\beta + \delta} \mathbf{D}_\lambda^\top \mathbf{D}_\lambda\right] z_4 + \frac{\delta}{\beta + \delta} \mathbf{D}_\lambda^\top p$ 
33:    end if
34:     $u \leftarrow (\mathbf{M}^\top \mathbf{M})^{-1} \mathbf{M}^\top \left(\frac{\lambda}{\beta} + y\right)$ 
35:     $\lambda \leftarrow \lambda + \beta(y - \mathbf{M}u)$ 
36:  end while
37:  return  $u$ 
38: end procedure

```

In the procedure, the vectors $\mathbb{1}$ and matrices Id are vectors of ones and identity matrices. Their dimensions depend on the context. $\forall k \in \{1, 2, 3\}$, $y_k = [y_{k,1}^\top, \dots, y_{k,L}^\top]^\top$ and $\lambda_k = [\lambda_{k,1}^\top, \dots, \lambda_{k,L}^\top]^\top$ such that $\forall l \in \{1, \dots, L\}$, $\forall k \in \{1, 2\}$, $y_{k,l}, \lambda_{k,l} \in \mathbb{R}^N \times \mathbb{R}^N$ and $y_{3,l} \in \mathbb{R}^N$. We define $\lambda = [\lambda_1^\top, \dots, \lambda_4^\top]^\top$. We can note that the operator $\mathbf{G} : \mathbb{R}^{LN} \rightarrow \mathbb{R}^N$ can be decomposed as:

$$\mathbf{G} = \mathbf{D}_\lambda \mathbf{H}_\lambda$$

where $\mathbf{H}_\lambda : \mathbb{R}^{LN} \rightarrow \mathbb{R}^{LN}$ is a circulant matrix associated with a spatially invariant convolution kernel defined by the sensitivity spectral pattern of the panchromatic image and $\mathbf{D}_\lambda :$

q	β	γ	σ_p	$\sigma_{\bar{u}}$	#iter
4	1000	0.01	0.0001	0.0001	300 & 3000

TABLE I
PARAMETERS OF TVLCSP FOR THE TESTS ON THE CUPRITE SCENE.

$\mathbb{R}^{LN} \rightarrow \mathbb{R}^N$ is a spectral decimation operator.

Finally, we define the matrix

$$\mathbf{M} = [(\nabla\pi_1)^\top, \dots, (\nabla\pi_L)^\top, (\nabla\pi_1)^\top, \dots, (\nabla\pi_L)^\top, \mathbf{H}_s^\top, \mathbf{H}_\lambda^\top]^\top \quad (6)$$

The up-sampling operator $\uparrow: \mathbb{R}^{LM} \rightarrow \mathbb{R}^{LN}$ spatially up-samples a vectorized hyperspectral image by a factor q and the vector $\mathbb{1}$ is a vector of ones of suitable dimension. The multiplications and divisions are element-wise. The ADMM procedure introduces an internal parameter, denoted β , whose value impacts the convergence speed.

Note that the update rule of u (line 34 in the procedure) can be computed in the Fourier domain. More precisely, since \mathbf{M}^\top and $\mathbf{M}^\top\mathbf{M}$ are circulant matrices (as concatenation and summation of circulant matrices, respectively), the left product by \mathbf{M}^\top , the inversion of $\mathbf{M}^\top\mathbf{M}$ and the left product by $(\mathbf{M}^\top\mathbf{M})^{-1}$ can be performed in the Fourier domain.

matrix \mathbf{M} is a concatenation of circulant matrices (Eq. 6), each associated with a convolution-type operation either in the two spatial dimensions (case of all matrices in Eq. 6 but \mathbf{H}_λ^\top) or in the spectral dimension (case of \mathbf{H}_λ^\top). Thus, the left side product by \mathbf{M}^\top is in the Fourier domain. Additionally, $\mathbf{M}^\top\mathbf{M}$ is a summation of circulant matrices, which is also circulant so the left-product by its inverse can be computed in the Fourier domain too. Thus, line 34 of the procedure should be replaced by:

$$u = \mathcal{F}^{-1} \left(\frac{\mathcal{F}(\mathbf{M}^\top) \cdot \mathcal{F} \left(\frac{\lambda}{\beta} + y \right)}{\mathcal{F}(\mathbf{M}^\top\mathbf{M})} \right) \quad (7)$$

where \mathcal{F} and \mathcal{F}^{-1} represent the Fourier transform and its inverse, respectively.

Currently, the stop condition is a number of iterations but another approach could be based on the stationary of y , λ and u .

IV. EXPERIMENTAL RESULTS

We present here results of TVLCSP on AVIRIS [6] and simulated HypXim [7] data. We have first extracted a selection of the Cuprite scene (AVIRIS) which represents a mineral area. The 224-spectral band data has been preprocessed and simulated as follows. 1 - Absorption spectral bands have been removed (bands: 1 – 6, 106 – 114, 152 – 170 and 215 – 224) to get a reference high resolution hyperspectral image u_{ref} . 2 - A convex combination of the spectral bands of u_{ref} gives the simulated panchromatic data p . The weights are the coefficients of the vector $\mathbf{g} = [\frac{1}{80} \dots \frac{1}{80}]$. 3 - The low resolution hyperspectral image x has been obtained from Eq. 1 without noise and with \mathbf{H}_s representing an average filter.

The chosen algorithm parameters are given in Table I. Visual results are presented in Fig. 1.

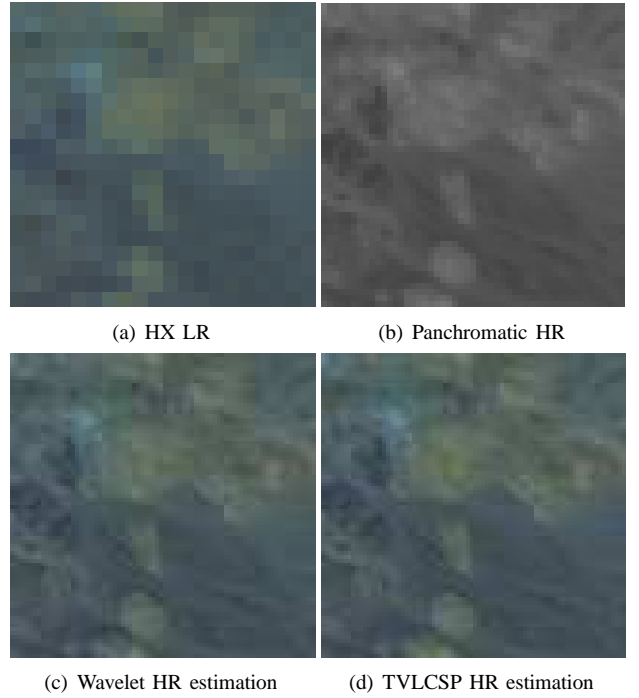


Fig. 1. Cuprite scene and processing with wavelet and TVLCSP, for a resolution ratio $q = 4$

	TVLCSP		Wavelet
	#300	#3000	
RMSE ($\times 100$)	0.48	0.59	0.91
ERGAS	5.45	6.68	10.3
SAM	0.61	0.70	0.88
FCC ($\times 100$)	99.3	99.0	99.1
D_s ($\times 100$)	1.15	0.89	2.35
D_λ ($\times 100$)	1.82	1.22	4.43

TABLE II
PERFORMANCES OF PAN-SHARPENING ALGORITHMS ON THE CUPRITE SUBIMAGE.

In Table II we present quantitative evaluation and comparison with a wavelet-based pan-sharpening method [1] using usual performance metrics: 1 - global quality metrics RMSE and ERGAS, 2 - spectral quality metrics SAM and the spectral dispersion the spatial dispersion D_λ [8]), and 3 - spatial quality metrics FCC [9] and spatial dispersion D_s [8]. Note that D_λ and D_s are metrics without reference (ground truth high resolution hyperspectral image) requirement, which is relevant where no reference is available or when the reference is likely to introduce error in comparison (case of our HypXim data) due to noise.

Additionally, TVLCSP has been tested on simulated HypXim data. They have been simulated from data acquired in the framework of the Pléiades program. The scene is located in Namibia and a sub-scene has been extracted. Some characteristics of the considered data are given in Table III. The considered sensitivity spectral pattern is shown in Fig. 2(a). We see that only some (20) of the spectral bands contribute to the panchromatic data thus only 20 non-zero coefficients in \mathbf{g} and the presented results only concerns these bands. Note that the hyperspectral sensor spatial Point Spread Functions (PSF) has been supposed Gaussian spectrally and spatially invariant,

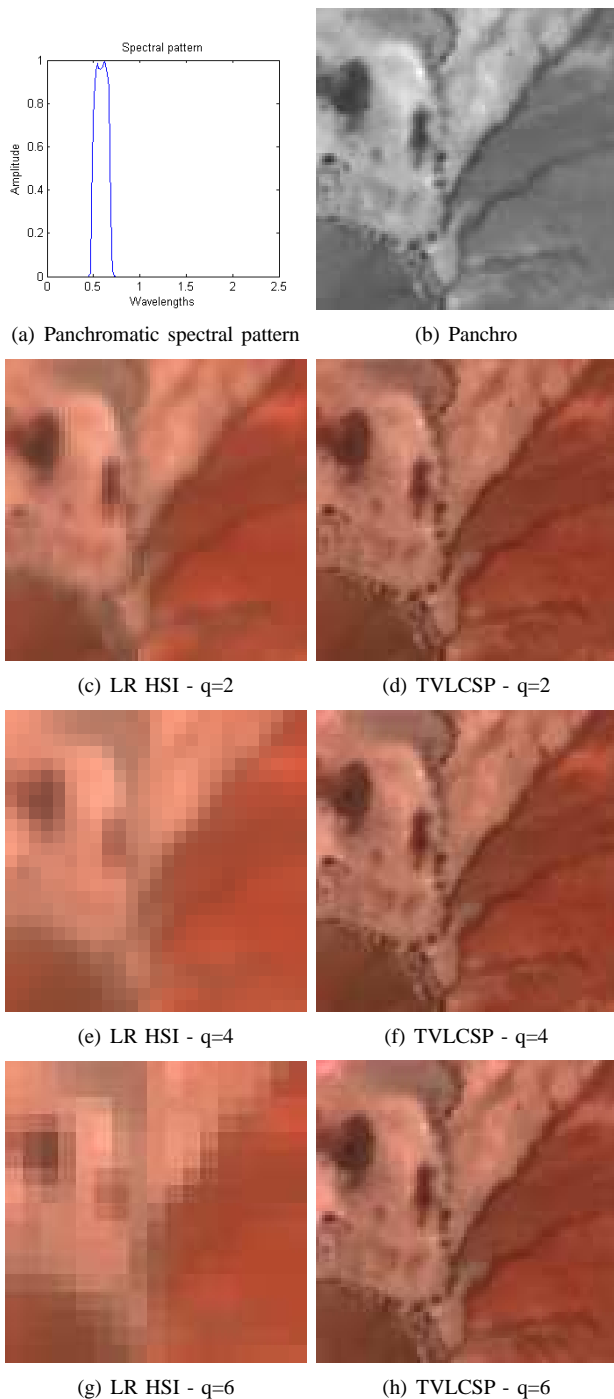


Fig. 2. HypXim scene and processing with TVLCSP, for resolution ratios $q = 2$ and $q = 6$.

q	Spatial resolution (m)	Simulated sensor
1	4.80	Panchromatic sensor
1	4.80	Reference
2	9.60	HypXim P (Performance concept)
4	19.20	HypXim C (Challenging concept)
6	28.80	ENMAP

TABLE III
CHARACTERISTICS OF THE SIMULATED HYPXIM AND PANCHROMATIC DATA.

	$q = 2$	$q = 4$	$q = 6$
RMSE $\times 100$	1.73	2.08	2.29
ERGAS	11.5	28.5	47.0
SAM	1.57	1.50	1.64
FCC $\times 100$	97.6	97.3	97.2
$D_s \times 100$	3.05	4.28	4.59
$D_\lambda \times 100$	3.41	2.30	1.82

TABLE IV
PERFORMANCES OF TVLCSP ON THE HYPXIM SUB-IMAGE

with a parameter tuned experimentally. The visual results are presented in Fig. 2 and the corresponding performance metrics are given in Table IV. We see that the method works well for many resolution ratios. However, the results on HypXim are not as good as those on AVIRIS, probably due to our approximation hypotheses on the sensor parameters and to the presence of noise. Note that the simulated reference image is corrupted by sensor noise whereas TVLCSP provides relatively denoised data estimations, which introduces lack of confidence in the performance metrics values.

V. CONCLUSION

We have tackled the pan-sharpening problem using a variational convex constrained approach with an objective based on the conservation of the set of iso-gray-level lines among spectral bands and total variation. The fit-to-data constraints have been mathematically considered as such and are based on the signal model and the sensor parameters, including noise statistics. An ADMM scheme has been developed, called TVLCSP and evaluated on AVIRIS and HypXim simulated data.

ACKNOWLEDGMENT

To cite this work, please use the reference [10]. The authors would like to thank the CNES for initializing and funding the study and providing HypXim simulated data.

REFERENCES

- [1] T. Ranchin and L. Wald, "Fusion of high spatial and spectral resolution images: the arsis concept and its implementation," *PERRS*, vol. 66, no. 1, pp. 49–61, 2000.
- [2] C. Ballester, V. Caselles, L. Igual, and J. Verdera, "A variational model for p+xs image fusion," *IJCV*, vol. 69, no. 1, p. 4358, 2006.
- [3] M. Joshi and A. Jalobeanu, "MAP estimation for multiresolution fusion in remotely sensed images using an IGMRF prior model," *IEEE TGRS*, vol. 48, no. 3, pp. 1245–1255, 2010.
- [4] V. Caselles, B. Coll, and J.-M. Morel, "Geometry and color in natural images," *JMIV*, vol. 16, no. 2, pp. 89–105, 2002.
- [5] L. Rudin, S. Osher, and E. Fatemi, "Nonlinear total variation based noise removal algorithms," *Physica D*, vol. 60, no. 1-4, pp. 259–268, 1992.
- [6] "Avisir," <http://avisir.jpl.nasa.gov/>.
- [7] R. Marion, V. Carrere, S. Jacquemoud, S. Chevrel, P. Prastault, M. D'oria, P. Giloupe, S. Hosford, B. Lubac, and A. Bourguignon, "Hypxim: A new hyperspectral sensor combining science/defence applications," in *WHISPERS*, 2011.
- [8] L. Alparone, B. Aiazzi, S. Baronti, A. Garzelli, F. Nencini, and M. Selva, "Multispectral and panchromatic data fusion assessment without reference," *PERRS*, vol. 74, no. 2, pp. 193–200, 2008.
- [9] Z. Zhou, D. Civico, and J. Silander, "A wavelet transform method to merge landsat TM and SPOT panchromatic data," *IIRS*, vol. 19, no. 4, 1998.
- [10] A. Huck, F. de Vieilleville, P. Weiss, and M. Grizonnet, "Hyperspectral pan-sharpening: a variational convex constrained formulation to impose parallel level lines, solved with ADMM," in *WHISPERS*, 2014.